Research Square

Preprints are preliminary reports that have not undergone peer review.
They should not be considered conclusive, used to inform clinical practice,
or referenced by the media as validated information.

Influence of Overburden Pressure on Grouting Flocculation– Vacuum Preloading

Yicun Wang
Beijing Urban Construction Survey & Design Research Institute Co., Ltd., Beijing
Diangan Chen
Beijing Urban Construction Survey & Design Research Institute Co., Ltd., Beijing
Weiwei Tang
tangweiwei002@163.com

College of Architecture and Civil Engineering, Wenzhou University, Wenzhou
Junfeng Ni
College of Architecture and Civil Engineering, Wenzhou University, Wenzhou
Mintao Xu
College of Architecture and Civil Engineering, Wenzhou University, Wenzhou
Zongfen Zhang
College of Architecture and Civil Engineering, Wenzhou University, Wenzhou

Research Article

Keywords: Soft ground improvement, Overburden pressure, Grouting flocculation, Vacuum preloading

Posted Date: November 26th, 2026

DOI: https://doi.org/10.21203/rs.3.rs-11440427/v1

License: This work is licensed under a Creative Commons Attribution 4.0 International License.
Read Full License

Additional Declarations: No competing interests reported.

Influence of Overburden Pressure on Grouting Flocculation–Vacuum Preloading

Yicun Wang[1,2], Diangan Chen[1,2], Weiwei Tang[3,4*], Junfeng Ni[3,4], Mintao Xu[3,4], Zongfen Zhang[3,4]

[1]1Beijing Urban Construction Survey & Design Research Institute Co., Ltd., Beijing 100084, China

[2]Beijing Key Laboratory of Deep Foundation Pit Geotechnical Engineering of Rail Transit,Beijing 100101, China

[3]College of Architecture and Civil Engineering, Wenzhou University, Wenzhou 325035, China

[4]Key Laboratory of Engineering and Technology for Tideland Reclamation and Life-Cycle Intelligent Monitoring of Zhejiang Province, Wenzhou, Zhejiang 325035, China

*Corresponding author: Weiwei Tang. E-mail: tangweiwei002@163.com

ABSTRACT

Grouting-flocculation vacuum preloading represents an innovative soft ground improvement technique.The grout diffusion range is governed by the overburden pressure, which leads to varying flocculation effects at different depths and further exerts influences on vacuum consolidation performance.To clarify the impact of overburden pressure on grouting flocculation-vacuum preloading, this paper conducted laboratory model tests of grouting flocculation under different overburden pressures and determined the effective range of grouting flocculation by measuring the total salt content of the soil. Subsequently, vacuum preloading tests were performed to evaluate the vacuum consolidation

effectiveness of dredged silt under different effective ranges. The results show that an increase in overburden pressure significantly inhibits the grout diffusion radius. The greater the pressure, the smaller the diffusion radius. When the pressure was 0 kPa, the maximum grouting radius reached 41 cm. As the pressure gradually increased to 80 kPa, the diffusion radius progressively decreased to 28 cm. Meanwhile, the largest grouting diffusion radius corresponded to the best vacuum consolidation effect. As the grouting flocculation radius decreased, the maximum reductions in mass of drained water and settlement during vacuum consolidation were approximately 7.68% and 6.29%, respectively. The moisture content increased by up to about 6.61%, and the vane shear strength decreased by a maximum of about 37.1%. Therefore, it is recommended that grouting under higher overburden pressures should adjust grouting parameters to expand the effective radius, thereby enhancing the effectiveness of grouting flocculation-vacuum preloading.

Keywords:Soft ground improvement;Overburden pressure; Grouting flocculation; Vacuum preloading

INTRODUCTION

In recent years, with the growing demand for intensive utilization of land resources, the efficient and eco-friendly treatment of dredged sludge has become an important research topic in geotechnical engineering. As an economical and effective soft soil improvement technology based on the drainage consolidation theory, vacuum preloading has been widely adopted at home and abroad (Qin et al. 2026; Tang and Shang 2000; Feng

et al. 2026). Nevertheless, clogging readily occurs when this method is applied to soft soils with high water content, which deteriorates the ground improvement efficiency (Feng et al. 2026; Cai 2021). Especially for soils with high initial water content and strong flowability, soil particles tend to migrate radially with pore water under negative pressure and rapidly form soil columns, further aggravating the clogging issue (Lei et al. 2025).

To improve this situation, numerous scholars have made technical improvements to the traditional vacuum preloading method (Shen et al. 2025; Wu and Wang 2010; Sun et al. 2025; Anda et al. 2023). Among these, the flocculation-vacuum preloading method involves adding flocculants to the soil, compressing the diffuse double layer around soil particles, and promoting the formation of flocculated structures, thereby effectively alleviating clogging and enhancing vacuum consolidation efficiency (Cao et al. 2026). Pu et al. (2020) conducted comparative vacuum preloading tests using PVD and PHD under conditions with added flocculants, concluding that PHD offers advantages such as faster drainage rate and better improvement effect for treating dredged silt. Hu et al.(2018) used $Ca(OH)_2$ and APAM to treat drilling waste slurry, and through one-dimensional consolidation tests, screened out the optimal dosages of 0.8% and 11.2% respectively based on indicators such as void ratio, permeability, and consolidation coefficient. Under the optimal dosage, $Ca(OH)_2$ performed best in vacuum preloading tests. Cai (2021) further optimized the vacuum consolidation effect by using a composite flocculation method of $Ca(OH)_2$+APAM and applied it to field soft ground improvement. The results showed that this method significantly shortened the treatment period and exhibited good

uniformity along the depth direction, although the composite flocculant has a greater impact on the environment.

However, flocculation is usually achieved by pipeline mixing, which is not suitable for existing foundations (Cao et al. 2024). Therefore, this study adopts the grouting flocculation-vacuum preloading method. In this method, grouting is used to cause a chemical reaction between the flocculant slurry and the soil in the existing soft ground, improving permeability and thus enhancing the consolidation efficiency of vacuum preloading (Wang et al. 2018). However, the diffusion radius of grouting is key to determining the improvement effect of vacuum preloading. The grout diffusion radius is mainly controlled by two types of factors: one is construction process parameters, such as grouting pressure and lifting rate, which directly control the diffusion process of the slurry. Wang and others (2025) used a pressure regulator to control grouting pressure and conducted laboratory model tests. By monitoring the changes in mass of drained water and settlement of sludge during vacuum preloading, combined with tests of soil moisture content and vane shear strength after improvement, they systematically analyzed the influence pattern of grouting pressure on the consolidation effect of vacuum preloading. Changchen and others (2026) treated dredged silt using different grouting pipe lifting rates and determined the optimal operating rate. A suitable lifting rate facilitates the dissipation of pore water pressure and improves consolidation efficiency. The second factor is stratigraphic conditions, especially soil moisture content and depth. Wang and others (2025) determined the optimal lime dosage for soils with different moisture contents and

applied it to the Longwan Phase II coastal wetland ecological restoration project. In that study, lime slurry was injected into dredged silt by grouting, effectively triggering flocculation reactions, increasing the soil permeability coefficient, thereby improving drainage efficiency during vacuum preloading, and ultimately enhancing the improvement effect. The influence of soil depth is mainly due to the difference in overburden pressure leading to variations in grouting effect. Especially during deep grouting, higher grouting pressure must be applied to overcome the greater vertical stress due to increased overburden pressure (Sun and Zhang 2019). Therefore, grouting at different depths requires different magnitudes of grouting pressure. However, in the grouting flocculation-vacuum preloading process, the effect of grouting is still unclear, and the influence of overburden pressure on grouting is not yet known, necessitating systematic research.

This paper investigates the slurry diffusion radius in sludge under different overburden pressure conditions through laboratory model tests and measures the corresponding changes in total salt content of the soil. On this basis, flocculation-vacuum preloading combined improvement is carried out on sludge samples with different slurry diffusion radius. During the improvement process, the changes in vacuum pressure, mass of drained water, and settlement are monitored. After improvement, the soil moisture content and vane shear strength are measured. The influence of the slurry diffusion radius on the treatment effect of grouting flocculation-vacuum preloading is systematically analyzed, aiming to provide a theoretical basis and technical reference for relevant

engineering practices.

LABORATORY MODEL TESTS

Test Soil Samples and Materials

Dredged silt was collected from the Longwan Phase II Coastal Wetland Restoration Project in Wenzhou, China. The retrieved material was homogenized, and water was added to obtain a pre-grouting water content of 110% (water mass divided by dry-soil mass). The soil-water mixture was stirred until visually homogeneous. Basic physical properties were measured in accordance with GB/T 50123-2019. The measured bulk density, specific gravity of soil solids, liquid limit, and plastic limit were 1.54 g/cm³, 2.72, 50.2%, and 23.5%, respectively; the initial vane shear strength was approximately zero because the material behaved as a slurry. The measured properties are summarized in Table 1.

TABLE1. Basic physical parameters of dredged silt

Bulk density (g/cm^3)	Initial water content (%)	Specific gravity of solids, G_s	Liquid limit, w_L (%)	Plastic limit, w_P (%)	Initial vane shear strength (kPa)
1.54	110	2.72	50.2	23.5	≈0

The particle-size distribution of the dredged silt was determined using a laser particle-size analyzer, and the resulting curve is presented in Figure 1. All particles had diameters smaller than 75 μm, while particles finer than 5 μm accounted for approximately 30% of the sample. Together with the basic physical properties, these results indicate that the dredged silt had a high water content and was predominantly composed of fine silt- and clay-sized particles.

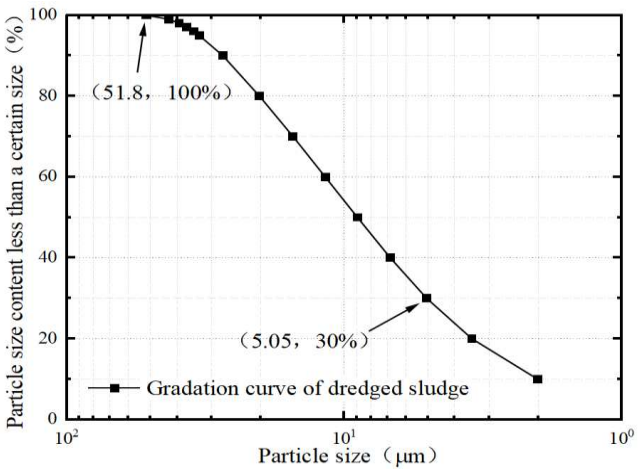

Fig.1. Particle size distribution curve of dredged silt

Considering the overall treatment performance, required dosage, and material cost, hydrated lime was selected as the flocculant in this study. The hydrated lime was purchased from Shanghai Zhanyun Chemical Co., Ltd. Its principal component was $Ca(OH)_2$, with a purity of no less than 95.0% and a molecular weight of 74.09 g mol^{-1}. Upon dissolution, Ca^{2+} ions can exchange with the monovalent cations associated with the soil particles. This process compresses the diffuse double layer and reduces the electrostatic repulsion between particles, thereby promoting particle aggregation and flocculation. The resulting aggregates can increase the hydraulic conductivity of the soil and accelerate slurry settling and dewatering.

Test Apparatus

The experimental setup consisted of a grouting system and a vacuum-preloading system, as shown in Figures 2 and 3. The grouting system mainly comprised an air compressor, a pneumatic diaphragm pump, a pressure-regulating valve, a slurry reservoir,

a grouting pipe, a cylindrical model tank, and air and slurry delivery lines.

The air compressor provided the compressed air required to drive the grouting system. It had a power rating of 550 W, a maximum pressure of 0.7 MPa, and an air-delivery rate of 40 L min^{-1}. A pressure-regulating valve with an adjustable range of 0.01–0.8 MPa was installed downstream of the compressor to regulate the air pressure supplied to the diaphragm pump and control the grouting pressure. The diaphragm pump had a flow rate of 0–1 m^3 h^{-1}, a maximum head of 50 m, and a suction lift of 0–5 m. Driven by compressed air, the diaphragm operated reciprocally, alternately increasing and decreasing the pump-chamber volume and continuously conveying slurry from the reservoir to the grouting pipe. The grouting pressure was controlled by the regulated air pressure and was also affected by the pump operating conditions and the flow resistance of the slurry-delivery line.The grouting pipe was an aluminum–plastic composite pipe with a length of 100 cm and an inner diameter of 1.2 cm. The pipe was equipped with a circular nozzle having an opening diameter of 0.3 cm. The model tank was made of acrylic, with a wall thickness of 1 cm and a diameter of 60 cm. Its top cover was fitted with linear bearings to guide the grouting pipe, maintain its injection direction, and control its lifting rate. To prevent slurry splash and leakage, two layers of geotextile together with a geomembrane were installed inside the model tank during the tests.

The vacuum-preloading system mainly consisted of a vacuum jet pump with a working pressure of 4 MPa, an integrated drainage plate, a vacuum gauge, a gas–water separator, an electronic balance, and air and water delivery lines. An integrated drainage

plate was used because it provides more effective vacuum transmission and drainage performance than conventional drainage plates. The drainage plate was 10 cm wide and 0.4 cm thick. During vacuum preloading, the vacuum pressure, cumulative drained-water mass, and settlement were monitored. After vacuum preloading, the soil water content and vane shear strength were measured.

Test Scheme

The tests aimed to investigate the grout-diffusion radius under different overburden pressures and to evaluate the consolidation performance of the combined flocculation–vacuum preloading method. Four model tests were conducted under overburden pressures of 0, 20, 40, and 80 kPa. The corresponding groups were designated T4, T3, T2, and T1, respectively. The grouting pressure was maintained at 0.5 MPa, and the lifting rate of the grouting pipe was 35 cm min^{-1}. The detailed test program is presented in Table 2.

TABLE 2. Experimental Scheme

Group	Overburden Pressure (kPa)	Soil Moisture Content (%)	Grouting Pressure P (MPa)	Water-to-Lime Ratio
T1	80	110	0.5	7:1
T2	40	110	0.5	7:1
T3	20	110	0.5	7:1
T4	0	110	0.5	7:1
ungrouted soil	0	110	0	0

Grouting Slurry Diffusion Radius Influence Test

(1) Place a layer of geotextile inside the model barrel to protect the geomembrane from scratching during the test. Then install the geomembrane to prevent sludge leakage and ensure adequate sealing for vacuum preloading. Finally, slowly pour the thoroughly mixed dredged sludge into the barrel until the soil layer reaches the predetermined height of 50 cm.

(2) Secure the lid, which is equipped with linear bearings and vent holes, to the model barrel using screws. The bearings were used to guide the grouting pipe and maintain the prescribed grouting direction and lifting rate. The air compressor, slurry reservoir, diaphragm pump, and grouting pipe were then connected.

(3) Different overburden pressures were applied to the soil surface using air pressure supplied by a booster pump. To transmit the air pressure effectively and prevent direct contact between the pressurized air and the soil, a latex film was first placed on the geomembrane. A 1–2 cm layer of clean water was then added above the latex film to form a uniform pressure-transfer layer. The grouting operation was subsequently carried out.

(4) Immediately after grouting, sludge samples were collected at different depths along the grouting direction at 5 cm intervals. The samples were dried and gently disaggregated. A 20 g portion of each sample was mixed with 100 mL of distilled water, stirred, and filtered. The filtrate was evaporated to dryness, and the residue was treated

with H_2O_2 and dried to constant mass. The total salt content was then calculated, and its variation along the grouting direction was used to determine the grout-diffusion radius.

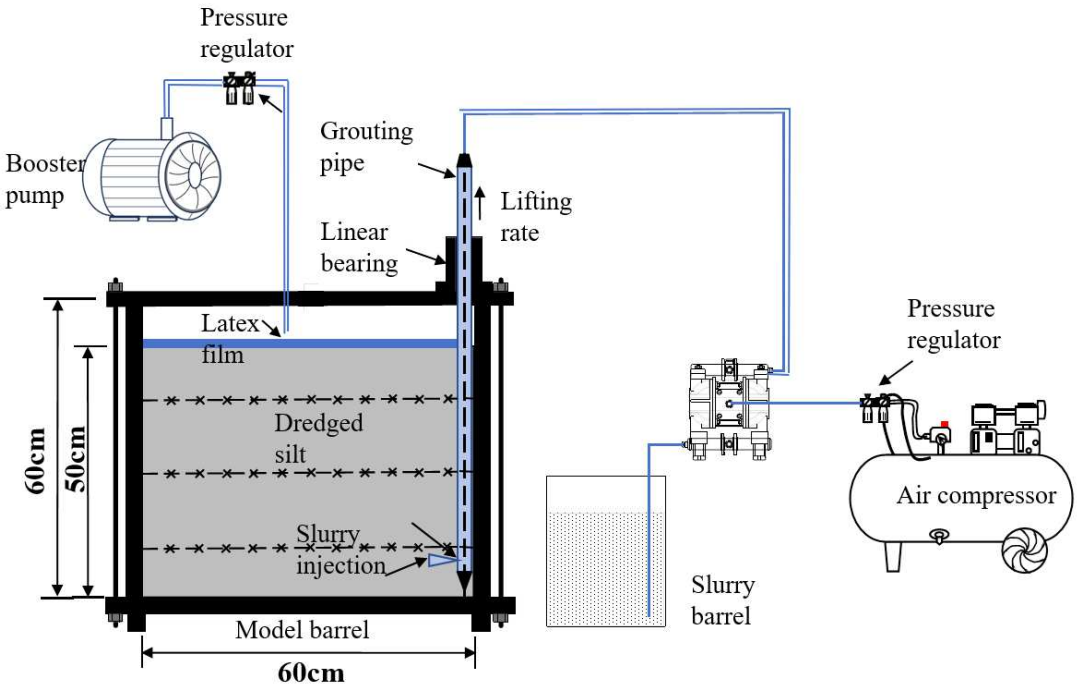

Fig. 2. Model diagram of grouting device

Flocculation Vacuum Preloading Consolidation Test

(1) Based on the test results of the slurry diffusion radius, we first determine the factor most significantly affecting the diffusion radius. Subsequently, conduct vacuum consolidation tests targeting this factor.

(2) After grouting, the treated soil was allowed to rest for 48 h. The grouting pipe was then removed, and the integrated drainage plate and monitoring instruments were installed. The drainage plate was connected to the gas–water separation bottle, which was in turn connected to the vacuum pump.

(3) The soil surface was covered with a geomembrane and sealed with glass

adhesive. The system was checked for leakage before vacuum loading.

(4) Vacuum preloading was then initiated. The vacuum degree beneath the geomembrane was maintained at no less than 80 kPa. The nominal drainage path was soil → drainage plate → connecting tube → gas–water separation bottle. The vacuum degree, cumulative discharged-water mass, and surface settlement were recorded throughout the treatment.

(5) When the monitored variables approached a stable state, the vacuum pump was stopped. Soil samples were then collected from the designated monitoring points to determine the water content, and the vane shear strength was measured at the corresponding depths.

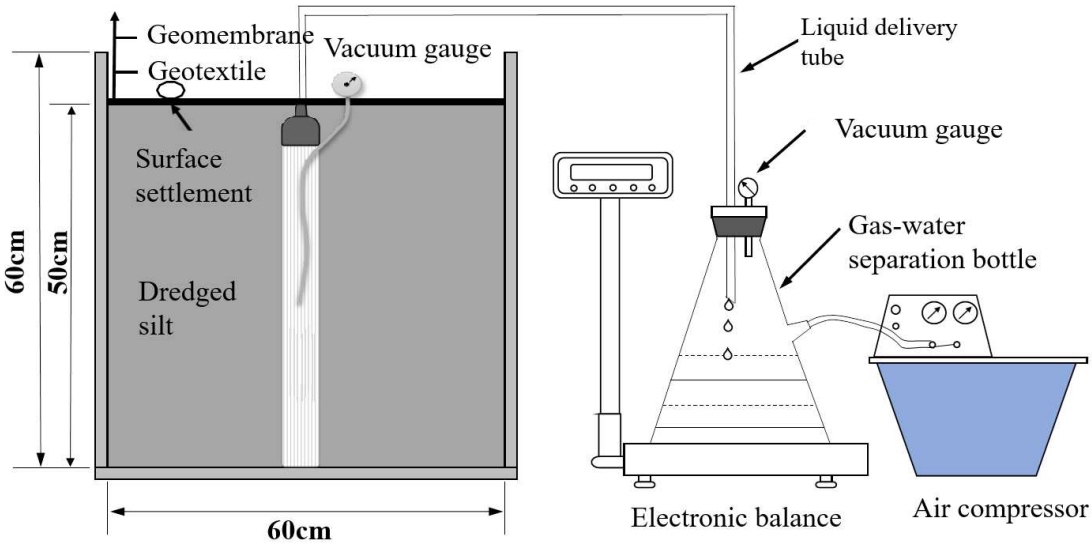

Fig. 3. Model diagram of vacuum preloading device

Test Monitoring and Measurement

To determine the grout-diffusion radius, a dedicated sampling and detection

procedure was developed based on the total salt content of the soil after grouting. Soil samples were collected using a sampler at 5 cm intervals along the grouting direction at depths of 10, 25, and 40 cm. When a sharp change in total salt content was observed between two adjacent sampling points, additional samples were collected at 1 cm intervals within that 5 cm interval. The specific sampling locations are shown in Figure 4.

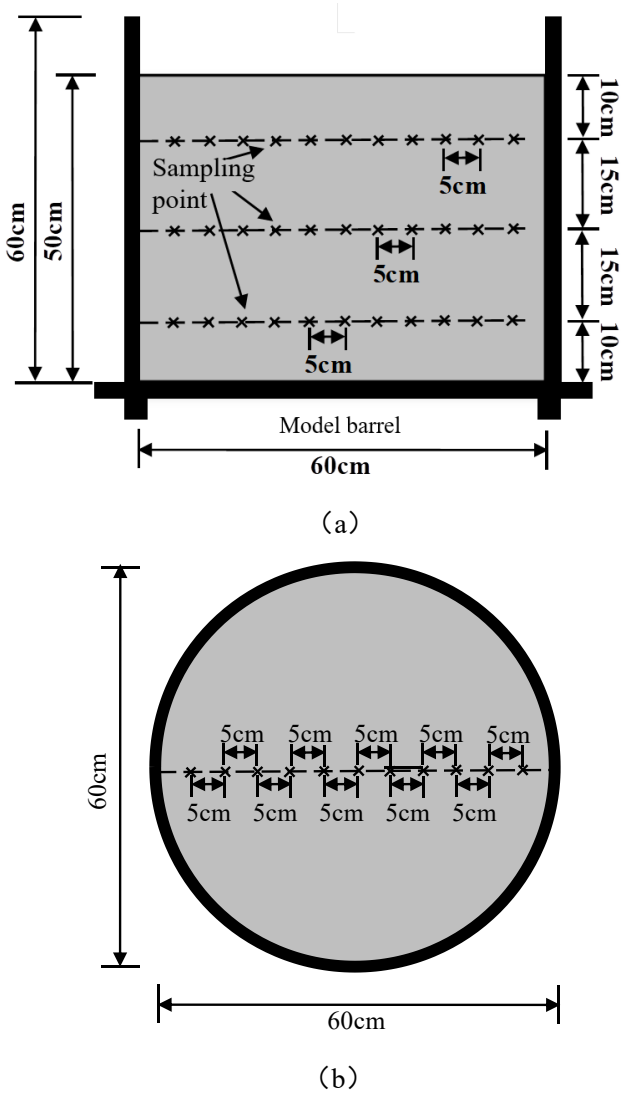

Fig. 4. Sampling point diagrams: (a) side view; (b) top view

To investigate the effect of the slurry-diffusion radius on the performance of grouting-assisted flocculation and vacuum consolidation of dredged sludge, a monitoring

system was established. The system was used to measure the vacuum pressure, mass of drained water, and settlement during vacuum preloading, as well as the soil water content and vane shear strength after treatment. Figure 5 shows the layout of the monitoring points for the vacuum-preloading tests.

The key parameters were monitored using the following methods. Vacuum pressure was measured at monitoring points beneath the geomembrane and at depths of 15 and 30 cm along the drainage plate. The mass of drained water was determined by weighing the gas–water separation device. Settlement was measured using surface markers and a graduated scale.

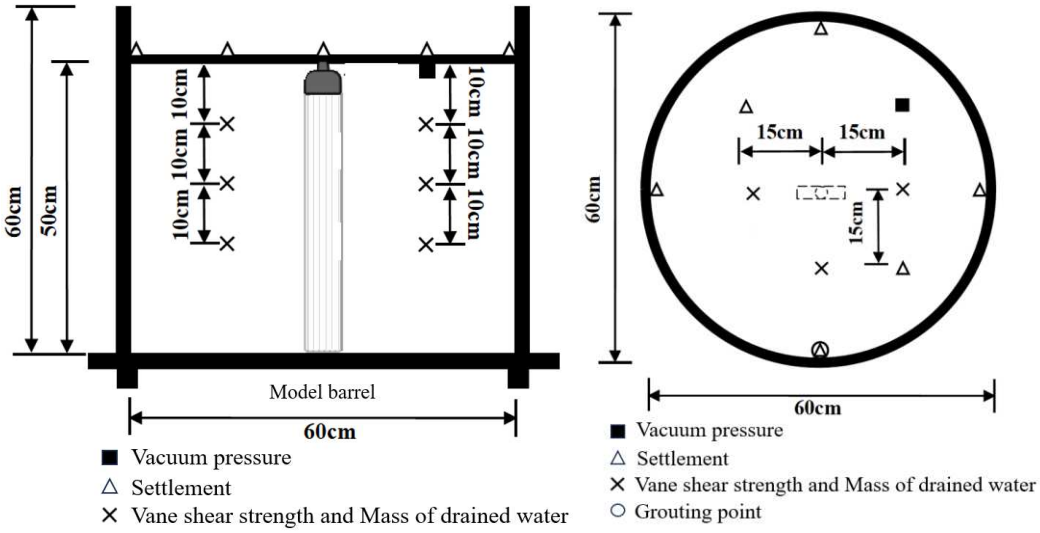

Fig. 5. Layout of vacuum preloading monitoring points: (a) side view; (b) top view

TEST RESULTS AND ANALYSIS OF GROUTING SLURRY DIFFUSION RADIUS

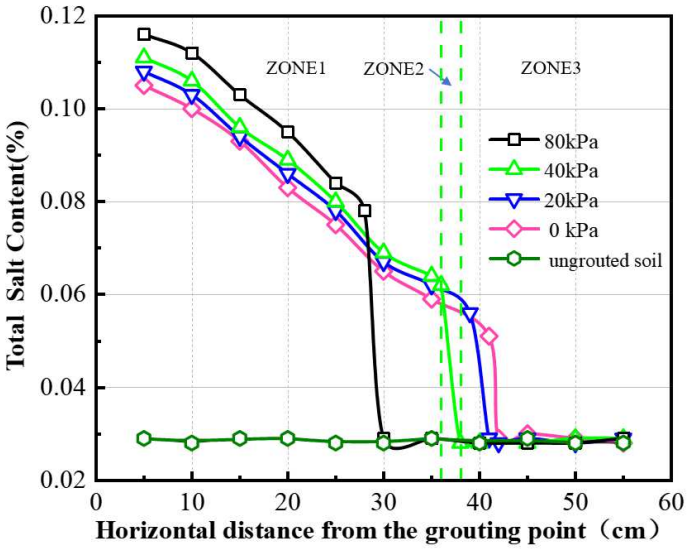

Fig. 6. Variation of total salt content with horizontal distance from the grouting point under different overburden pressures

The variation in the total salt content of the soil with horizontal distance from the grouting point under different overburden pressures is shown in Figure 6. The distance over which the total salt content was elevated gradually decreased as the overburden pressure increased, indicating a reduction in the grout-diffusion radius. The distribution of the total salt content can be divided into three regions.For example, under the 40-kPa overburden-pressure condition, Region 1 extended from 5 to 36 cm from the grouting point. In this region, the total salt content gradually decreased with increasing horizontal distance but remained relatively high overall. This elevated salt content was attributed to both the $Ca(OH)_2$ introduced with the grout and the naturally occurring salts in the sludge.Region 2 extended from 36 to 38 cm, where the total salt content decreased

sharply. This sharp change indicates the transition between the grout-affected and unaffected zones. Therefore, the grout-diffusion radius was defined as approximately 36 cm.Region 3 extended from 38 to 55 cm. In this region, the total salt content remained nearly constant and was close to that of the untreated sludge. This result indicates that the injected $Ca(OH)_2$ grout had little or no influence in this region. Similar distribution patterns were observed for the other test groups, and their grout-diffusion radii were determined using the same criterion.

Based on these results, the relationship between the slurry-diffusion radius and overburden pressure is presented in Figure 7. The slurry-diffusion radius gradually decreased as the overburden pressure increased. Within the tested range, overburden pressure exerted a clear influence on the slurry-diffusion radius. A fitting relationship between the slurry-diffusion radius (R) and the overburden pressure (P_o) was established, and the resulting equation is given as Eq. (1).

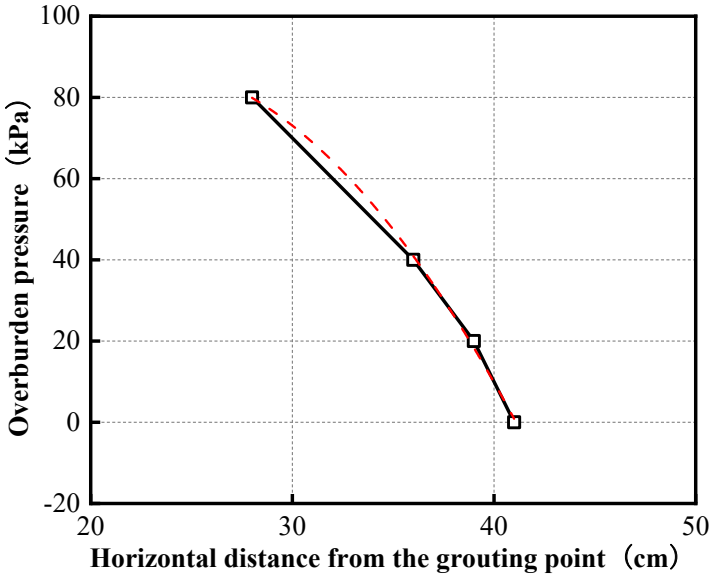

Fig. 7. Variation curve of slurry diffusion radius with overburden pressure

$$P_o=-0.24R^2+10.59R-27.21 \quad (1)$$

Here, the slurry-diffusion radius (R) and the overburden pressure (P_o) are the key variables in the model. As (P_o) increased from 0 to 40 kPa, the slurry-diffusion radius decreased gradually, with a reduction rate of approximately 6.9%. When (P_o) exceeded 40 kPa, the reduction rate increased to approximately 12.2%, indicating that the slurry-diffusion radius became more sensitive to the overburden pressure. Therefore, 40 kPa may represent a transition point at which the influence of overburden pressure on the slurry-diffusion radius becomes more pronounced within the tested range.

VACUUM PRELOADING TEST RESULTS AND ANALYSIS

Vacuum Pressure under Different Overburden Pressures

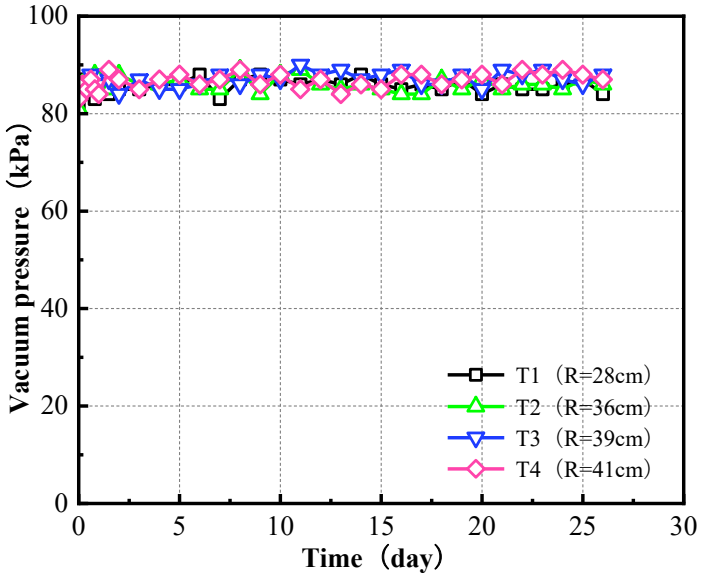

Fig. 8. Variation of vacuum pressure beneath the membrane with time

The temporal variation in the measured vacuum pressure provides information on vacuum transmission and the hydraulic response of the treated dredged sludge. The vacuum-pressure curves obtained during the tests are presented in Figure 8. Immediately after vacuum application began, the vacuum pressure increased rapidly to approximately 85 kPa and subsequently remained within 84–90 kPa. This initial increase likely reflects the establishment of vacuum in the drainage system and the transient pore-pressure response. The subsequent stabilization indicates that the sealing system and drainage path reached a relatively steady operating state. Because the vacuum pressure remained similar among the test groups, Figure 8 alone does not demonstrate an independent effect of the slurry-diffusion radius on consolidation performance.

Mass of Drained Water under Different Overburden Pressures

The slurry-diffusion radius is an important parameter associated with the dewatering and consolidation response of dredged sludge treated by grouting-assisted flocculation and vacuum preloading. However, because the overburden pressure and slurry-diffusion radius varied simultaneously in the present tests, the results should be interpreted as a coupled response rather than as evidence of an independent effect of (R). The mass of drained water was quantified from the change in mass of the gas–water separation bottle during vacuum preloading. The corresponding curves of cumulative drained-water mass versus vacuum-preloading time are presented in Figure 9.All test groups exhibited two drainage stages: a rapid-drainage stage followed by a slow-drainage stage. The final cumulative drained-water mass was highest in T1 and lowest in T2, following the order T1 > T4 > T3 > T2. The slow-drainage stage began earlier in T2–T4 than in T1. This difference likely reflects the combined effects of grout distribution and stress history. Although all groups received the same nominal lime dosage, T1 was subjected to the highest overburden pressure (80 kPa) and had the smallest slurry-diffusion radius (28 cm). The higher overburden pressure produced greater compression and pore-water expulsion, while the smaller diffusion radius may have resulted in a less extensive and spatially less uniform treated zone. These factors could have altered the hydraulic resistance and delayed the transition to slow drainage in T1.Among T2–T4, the slow-drainage stage began earlier in T3 and T4 than in T2, and T4 showed a slightly larger final drained-water

mass than T3. This trend is consistent with the larger diffusion radii of T3 and T4, which may have promoted more extensive contact between the lime grout and the soil and improved drainage connectivity. Nevertheless, this interpretation represents an association rather than a confirmed causal relationship because the overburden pressure also differed among the test groups. Therefore, the final drained-water mass should be regarded as an indicator of the overall dewatering and volume-change response, rather than as a standalone measure of consolidation performance.

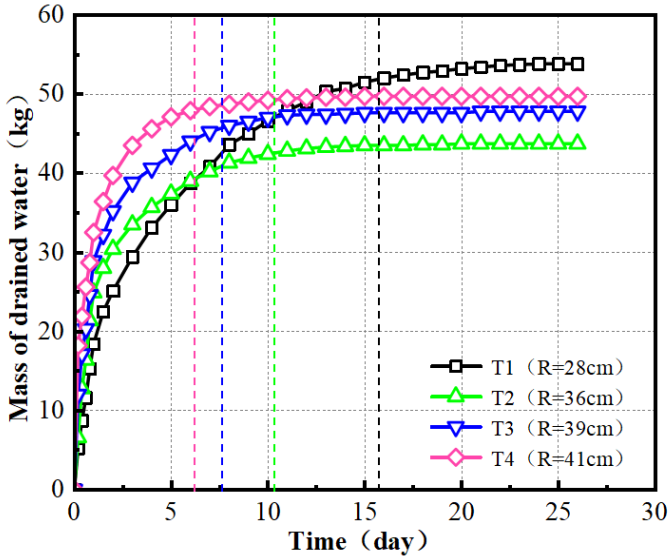

Fig. 9. Variation curve of mass of drained water over time

Settlement under Different Overburden Pressures

Surface settlement is an important indicator of the deformation and consolidation response of treated dredged sludge. In this study, settlement was monitored during vacuum preloading to assess the coupled effects of the slurry-diffusion radius and overburden pressure. The settlement curves are shown in Figure 10. The final settlement

magnitudes followed the order T1 > T4 > T3 > T2.The settlements of Groups T2, T3, and T4 stabilized earlier than that of Group T1. This difference should not be attributed to the absence of flocculation, because all groups received the same nominal lime dosage. T1 was subjected to the highest overburden pressure (80 kPa) and had the smallest slurry-diffusion radius (28 cm). The high overburden pressure generated excess pore-water pressure and caused consolidation compression as the pore pressure dissipated. The resulting stress history, together with the less extensive and less uniform grout distribution associated with the smaller diffusion radius, may have prolonged the settlement process.Among Groups T2–T4, the settlements of T3 and T4 stabilized earlier than that of T2, which may be related to their larger diffusion radii and more extensive soil–grout contact. However, because the overburden pressure and diffusion radius varied simultaneously, their independent effects cannot be separated. Therefore, the larger final settlement of T1 reflects a coupled response to overburden-induced consolidation, vacuum preloading, and grout-distribution heterogeneity, rather than poor flocculation or a direct measure of treatment performance.

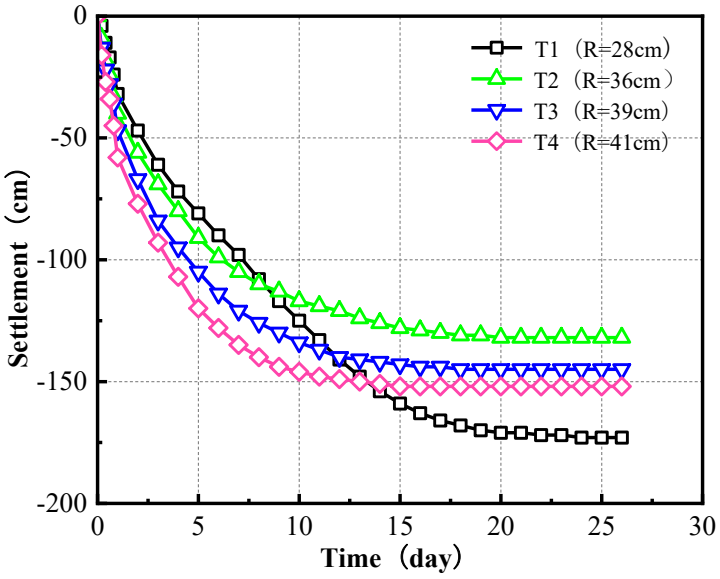

Fig. 10. Variation curve of soil surface settlement over time

Soil Moisture Content under Different Overburden Pressures

After vacuum preloading, soil samples were collected from the designated monitoring points using a sampler, and their water contents were determined in accordance with standard geotechnical testing procedures. The resulting water-content profiles with depth are presented in Figure 11. In general, the water content increased with depth. However, the final water content did not show a monotonic relationship with the slurry-diffusion radius.Group T1 had the largest overburden pressure on the soil, the smallest diffusion range, and the lowest degree of mixing with the soil, resulting in the slowest drainage rate during vacuum consolidation, but ultimately the smallest final soil moisture content. However, for Groups T2, T3, and T4, at the same depth, the soil moisture content showed an increasing trend. This is because lime reacts chemically with

pore water in the soil, generating a series of solid hydrated compounds,these solid hydrated compounds decompose after prolonged high-temperature drying in an oven, removing the bound water, presenting a phenomenon of higher moisture content compared to the same depth in Group T1. The final moisture content of Groups T3 and T4 was lower than that of Group T2. This is because the slurry diffusion range in the soil for Groups T3 and T4 was relatively large, and the degree of mixing with the soil was relatively high, forming stable drainage channels, resulting in a smaller final moisture content.

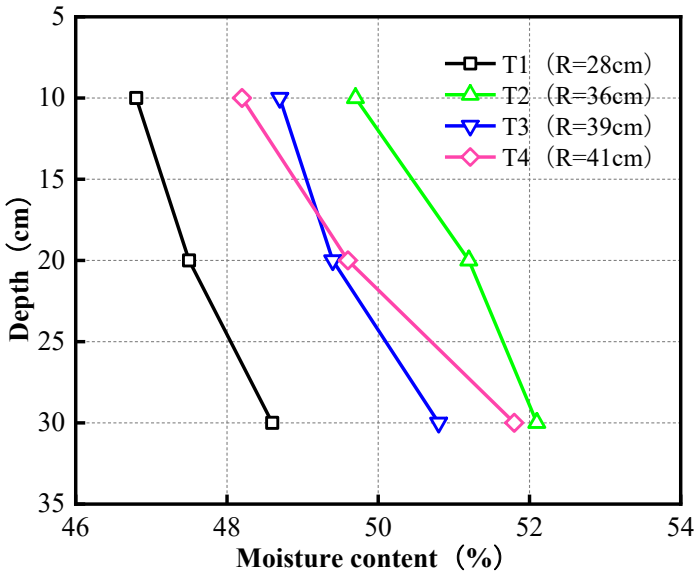

Fig. 11. Variation curve of soil moisture content along depth

Soil Vane Shear Strength under Different Overburden Pressures

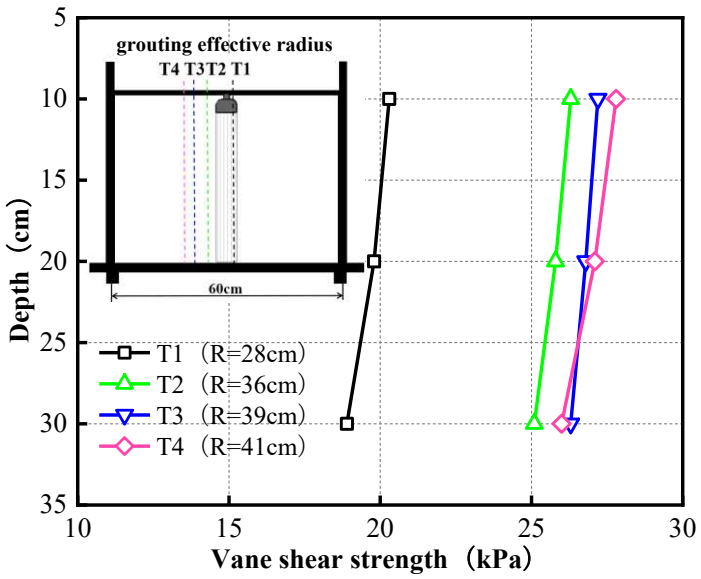

Fig. 12. Variation curve of soil vane shear strength along depth

After vacuum preloading, a portable vane shear tester was used to measure the vane shear strength of the treated soil at the designated monitoring points. The resulting depth profiles of vane shear strength are presented in Figure 12. In general, the vane shear strength of each test group decreased with increasing soil depth. Comparative analysis showed that Group T1 had the lowest average vane shear strength among all groups.Although T1 received the same nominal lime dosage as the other groups, it was subjected to the highest overburden pressure, which resulted in the smallest slurry-diffusion radius. This radius was smaller than the effective influence range of the drainage plate. Because the grouting point was located at the farthest end of the drainage plate's effective influence zone, the grout-affected zone in T1 may not have reached the

soil surrounding the drainage plate. Consequently, T1 may have been less effective in reducing local hydraulic resistance and clogging, which could have limited drainage and contributed to its lower final vane shear strength. However, this interpretation should be considered a possible mechanism, because the final strength was also affected by the effective stress, water content, consolidation degree, and lime-induced changes in soil fabric.

In contrast, as the overburden pressure decreased from T2 to T4, the slurry-diffusion radius increased accordingly. The grout-affected zones in these groups likely extended to the vicinity of the drainage plate, which may have reduced local hydraulic resistance and mitigated clogging. Accordingly, the treated soils exhibited higher vane shear strengths than Group T1.

CONCLUSIONS

This paper aims to study the influence of overburden pressure on grouting flocculation-vacuum preloading. Through grouting flocculation model tests combined with soil total salt content analysis, the effective diffusion radius of grouting flocculation under different overburden pressures was determined. Subsequently, vacuum preloading tests were conducted on the flocculated soil. By systematically monitoring and comparing the changes in vacuum pressure, mass of drained water, and settlement during the improvement process for each test group, combined with the test results of soil moisture content and vane shear strength after improvement, the influence of overburden pressure

on grouting flocculation-vacuum preloading was systematically explored, and the following conclusions were drawn:

（1）As the overburden pressure increases, the effective radius of grouting flocculation gradually decreases. When the pressure was 0 kPa, the maximum grouting radius reached 41 cm. As the pressure gradually increased to 80 kPa, the diffusion radius progressively decreased to 28 cm.

（2）The largest grouting diffusion radius corresponded to the best vacuum consolidation effect. As the effective grouting flocculation radius decreased from 41 cm to 28 cm, the maximum reductions in soil mass of drained water and settlement during vacuum consolidation were approximately 7.68% and 6.29%, respectively. The soil moisture content increased by up to about 6.61%, and the vane shear strength decreased by a maximum of about 37.1%.

In summary, overburden pressure significantly affects the grouting radius, thereby weakening the vacuum consolidation effect. Therefore, for grouting at greater depths, parameters such as grouting pressure should be increased to expand the influence radius of grouting.

DATA AVAILABILITY STATEMENT

Some or all data that support the findings of this study are available from the corresponding author upon reasonable request.

ACKNOWLEDMENTS

The authors thank the laboratory staff for their assistance with experimental preparation and data collection.

This work was supported by the National Natural Science Foundation of China (Grant No. 52408389) and the Basic Public Welfare Research Program of Zhejiang Province, China (Grant No. LTGG24E080004). Junfeng Ni received research support from these two grants. Mintao Xu received research support from the Wenzhou Basic Scientific Research Project (Grant No. S20240007).

DISCLAIMERS

The opinions, findings, and conclusions expressed in this paper are those of the authors and do not necessarily reflect the views of the supporting organizations.

NOTATIO NLIST

P_g = grouting pressure (MPa)

P_o = overburden pressure (kPa)

R = slurry-diffusion radius (cm)

REFERENCE

Anda, R. L., J. C. Chai, and T. Negami. 2023. “Effect of chemical additives on the consolidation behaviours of mini-PVD unit cells–from macro to micro.” Geotextiles and Geomembranes 51 (1): 199–208. https://doi.org/10.1016/j.geotexmem.2022.105647.

Cai, Y. Q. 2021. “Consolidation mechanism of vacuum preloading for dredged slurry and

anti-clogging method for drains." Chinese Journal of Geotechnical Engineering 43 (2): 201–225. (in Chinese).

Cao, X. L., H. T. Fu, Y. Peng, Z. F. Zhang, and M. M. Ge. 2024. "Experimental study on influence of grouting pressure on treatment effect of grouting flocculation-vacuum preloading." Shanxi Architecture 50 (16): 1–4. (in Chinese).

Cao, Y., J. Liu, Z. Qiu, X. Yong, and J. Yin. 2026. "Insights into the microstructural evolution of dredged clay treated by SAP flocculation and vacuum preloading." Engineering Geology 363: 108560. https://doi.org/10.1016/j.enggeo.2026.108560.

Changchen, Z., et al. 2026. "Influence of grouting pipe lifting rate on vacuum preloading performance for dredged sludge." Geotechnical and Geological Engineering 44 (1): 68–81. https://doi.org/10.1007/s10706-025-02117-7.

Chen, S., et al. 2026. "Efficient hydrogen storage in hydrate solid solution: structural insights and performance." International Journal of Hydrogen Energy 204: 153331. https://doi.org/10.1016/j.ijhydene.2026.153331.

Feng, J., Y. Shen, W. Qi, W. Shi, and H. Yang. 2026. "Numerical modelling of dredged sediment improvement under electrokinetic geosynthetics assisted vacuum preloading combined with electroosmosis." Geotextiles and Geomembranes 54 (1): 209–223. https://doi.org/10.1016/j.geotexmem.2025.105876.

Feng, X. 2025. "Foundation treatment forms for subgrade sections of Wenzhou urban railway under deep soft soil geological conditions." China Construction (9). (in Chinese).

Hu, T., Y. J. Wu, F. Xu, et al. 2018. “Effects of calcium hydroxide and polyacrylamide on the consolidation of high moisture content mud.” Journal of Yangtze River Scientific Research Institute 35 (8): 95–101. (in Chinese).

Lei, H., J. Li, S. Feng, T. Ma, G. Zhang, and S. Yu. 2025. “Reinforcement effectiveness of stacked prefabricated vertical drain (S-PVD) vacuum preloading method: a case study.” Geotextiles and Geomembranes 53 (6): 1266–1280. https://doi.org/10.1016/j.geotexmem.2025.106671.

Li, Z. H., and C. D. Wang. 2025. “Analysis of deformation influence of new urban railway subgrade on adjacent existing high-speed railway subgrade in deep soft soil areas.” Urban Mass Transit Research 28 (6). (in Chinese).

Liu, C. Y. 2023. “Safety assessment of EMUs for the first phase project of Wenzhou urban railway Line S1.” Urban Mass Transit Research 26 (6). (in Chinese).

Pu, H. F., Y. F. Pan, D. Khoteja, et al. 2020. “Model test on dewatering of high-water-content dredged slurry by flocculation-horizontal vacuum two-staged method.” Rock and Soil Mechanics 41 (5): 1502–1509. (in Chinese).

Qin, W., Y. Pan, G. Dai, X. Dong, and X. Du. 2026. “Lateral cyclic behaviors of piles installed in silt treated by vacuum preloading method (VPM) considering the one-way and two-way loading modes.” Soil Dynamics and Earthquake Engineering 203: 109986. https://doi.org/10.1016/j.soildyn.2026.109986.

Shen, Y., N. Wei, K. Fan, W. Qi, J. Feng, and Z. Lai. 2025. “Chemical-enhanced electrokinetic geosynthetics (EKG) electro-osmosis combined with vacuum

preloading for consolidation and copper remediation in contaminated dredged sludge." Geotextiles and Geomembranes 53 (6): 1600–1609. https://doi.org/10.1016/j.geotexmem.2025.106702.

Sun, Y., et al. 2025. "Study on the effect and mechanism of hot-air-boosted vacuum preloading solidification of dredged silt via model tests." Applied Ocean Research 161: 104684. https://doi.org/10.1016/j.apor.2025.104684.

Sun, Z. Q., and L. Zhang. 2019. "Experimental study on slurry diffusion radius under different grouting pressures." Coal Mine Modernization (5): 109–111. (in Chinese).

Tang, M., and J. Q. Shang. 2000. "Vacuum preloading consolidation of Yaoqiang Airport runway." Géotechnique 50 (6): 613–623. https://doi.org/10.1680/geot.2000.50.6.613.

Wang, J., R. Zhao, Y. Cai, H. Fu, X. Li, and X. Hu. 2018. "Vacuum preloading and electro-osmosis consolidation of dredged slurry pre-treated with flocculants." Engineering Geology 246: 123–130. https://doi.org/10.1016/j.enggeo.2018.09.013.

Wang, J., K. Y. Zhang, J. F. Ni, H. T. Fu, and Y. Peng. 2025. "Experimental study on consolidation of dredged slurry by grouting flocculation-vacuum preloading method considering influence of soil salinization." Chinese Journal of Geotechnical Engineering 47 (4): 801–810. (in Chinese).

Wu, M. Q., and B. Wang. 2010. "Comparative analysis of surcharge preloading and vacuum preloading in soft ground improvement." Chinese Journal of Geotechnical Engineering 29 (S1): 2916–2926. (in Chinese).